


Article

Improving DFT-Based Image Watermarking Using Particle Swarm Optimization Algorithm

Manuel Cedillo-Hernandez ¹, Antonio Cedillo-Hernandez ^{2,*}  and Francisco J. Garcia-Ugalde ³

¹ Instituto Politecnico Nacional SEPI ESIME Culhuacan, Av. Santa Ana 1000 Culhuacan CTM V, Mexico City 04440, Mexico; mcedilloh@ipn.mx

² Tecnologico de Monterrey, Escuela de Ingeniería y Ciencias, Av. Eugenio Garza Sada 2501, Monterrey 64849, Mexico

³ Facultad de Ingeniería, Universidad Nacional Autónoma de México, Avenida Universidad 3000 Ciudad Universitaria, Coyoacán, Mexico City 04510, Mexico; fgarciau@unam.mx

* Correspondence: acedillo@tec.mx; Tel.: +52-55-39540167

Abstract: Robust digital image watermarking is an information security technique that has been widely used to solve several issues related mainly with copyright protection as well as ownership authentication. In general terms, robust watermarking conceals a small signal called a “watermark” in a host image in a form imperceptible to human vision. The efficiency of conventional robust watermarking based on frequency domain depend directly on the results of performance in terms of robustness and imperceptibility. According to the application scenario and the image dataset, it is common practice to adjust the key parameters used by robust watermarking methods in an experimental form; however, this manual adjustment may involve exhaustive tasks and at the same time be a drawback in practical scenarios. In recent years, several optimization techniques have been adopted by robust watermarking to allowing adjusting in an automatic form its key operation parameters, improving thus its performance. In this context, this paper proposes an improved robust watermarking algorithm in discrete Fourier transform via spread spectrum, optimizing the key operation parameters, particularly the amounts of bands and coefficients of frequency as well as the watermark strength factor using particle swarm optimization in conjunction with visual information fidelity and bit correct rate criteria. Experimental results obtained in this research show improved robustness against common signal processing and geometric distortions, preserving a high visual quality in color images. Performance comparison with conventional discrete Fourier transform proposal is provided, as well as with the current state-of-the-art of particle swarm optimization applied to image watermarking.

Keywords: robust watermarking; information security; spread spectrum; ownership authentication; image processing; particle swarm optimization



Citation: Cedillo-Hernandez, M.; Cedillo-Hernandez, A.; Garcia-Ugalde, F.J. Improving DFT-Based Image Watermarking Using Particle Swarm Optimization Algorithm. *Mathematics* **2021**, *9*, 1795. <https://doi.org/10.3390/math9151795>

Academic Editor: Galina Bogdanova

Received: 25 June 2021

Accepted: 16 July 2021

Published: 29 July 2021

Publisher’s Note: MDPI stays neutral with regard to jurisdictional claims in published maps and institutional affiliations.



Copyright: © 2021 by the authors. Licensee MDPI, Basel, Switzerland. This article is an open access article distributed under the terms and conditions of the Creative Commons Attribution (CC BY) license (<https://creativecommons.org/licenses/by/4.0/>).

1. Introduction

Currently, most modern capturing equipment produces digital images in an easy and massive way. With the great growth of multimedia systems, the users have found novel ways to exchange and publish digital images without any restriction, mainly in social networks and on web sites. This behavior has increased the interest of scientific community in developing efficient methods to address copyright protection problems in recent decades [1–4]. Digital watermarking is an emerging technique that has been widely used by multimedia systems for improving aspects of information security related to ownership authentication and copyright protection. Conventionally, over time digital watermarking has been classified mainly in visible and invisible modalities, respectively. In general terms, digital watermarking methods embed information (i.e., a watermark) to create a trustworthy link between the watermark and the hosting object.

In the context of invisible watermarking, a technique of this modality is as efficient as the results of its evaluations regarding robustness and imperceptibility. Robustness is a measurement to evaluate if inserted binary data remains even after severe attacks are performed upon the watermarked image. Furthermore, in many applications, it is imperative to preserve almost the same visual quality as the original image to prevent any distortion perceptible by a naked eye. In this way, invisible watermarking is the most explored modality in scientific literature to find a solution to information security issues in digital images. This modality involves two stages. The first one embeds a signal called a “watermark” in an imperceptible manner, obtaining often high visual quality watermarked images. The second stage extracts and detects the watermark signal even though the protected images have experienced changes because of several image processing operations during its transmission or storage, either caused in an intentional or non-intentional manner, such as image compression, noise corruption, filtering, or geometric distortions, among others. The aim of invisible watermarking is detecting or extracting the watermark signal without any ambiguity, even if the image is severely distorted, i.e., the digital image watermarking algorithm should be as robust as possible against attacks that attempt to make difficult recovery tasks. The main capabilities of invisible watermarking are: (a) embed an invisible watermark pattern in the image content, (b) identify ownership, (c) high transparency image content, (d) high quality of watermarked image, (e) need for explicit extractor/detector, (f) high robustness, (g) often higher computational complexity and (h) versatility of media content.

Conventionally, invisible watermarking is performed in spatial, frequency or hybrid domains, in conjunction with advanced image and/or signal processing techniques to improve, as far as possible, the performance in terms of imperceptibility, capacity and robustness [1–4]. In this way, in recent years the scientific community has been focusing its attention in optimize the invisible watermarking methods via optimization algorithms, such as the particle swarm optimization (PSO) algorithm [5], among others.

Motivated and inspired by this trend, this paper proposes an improved robust invisible watermarking algorithm in discrete Fourier transform (DFT) via direct sequence code division multiple access (DS-CDMA) [6,7], optimizing the key operation parameters, particularly the amounts of bands and coefficients of frequency as well as the watermark strength factor, using the PSO algorithm in conjunction with visual information fidelity (VIF) and bit correct rate (BCR) criteria. Experimental results obtained in this research shows improved robustness against common signal processing and geometric distortions, preserving a high visual quality in color images. Performance comparison with the conventional discrete Fourier transform proposal is provided, as well as with the current state-of-the-art of PSO applied to invisible watermarking. The organization of the proposed paper is as follows. In Section 2 we explain the background, motivation, contribution, and a general description of this work. In Section 3 we explain in a detailed manner the proposed algorithm. Section 4 includes the experimental results and discussion. Finally, Section 5 concludes this work.

2. Background and Contributions

Since the beginning of the digital watermarking era [1,2], one of the most explored frequency domains into invisible watermarking field is the bidimensional DFT domain. The 2D DFT transform of an image $I(x,y)$ of size $N_1 \times N_2$ is given by (1):

$$F(u, v) = \sum_{x=1}^{N_1} \sum_{y=1}^{N_2} I(x, y) e^{-j2\pi(ux/N_1 + vy/N_2)}. \quad (1)$$

Some well-known properties of the DFT are that in the spatial domain they do not affect the magnitude of the 2D DFT transform, as shown in (2):

$$|DFT[I(x + x_1, y + y_1)]| = M(u, v), \quad (2)$$

where $M(u,v) = |F(u,v)|$ and x_1, y_1 are translation parameters. Concerning the scaling in the spatial domain it causes an inverse scaling in the frequency domain, as shown in (3):

$$DFT[I(\rho x, \rho y)] = \frac{1}{\rho} F\left(\frac{u}{\rho}, \frac{v}{\rho}\right), \quad (3)$$

where ρ is the scaling factor. Rotation in the spatial domain causes the same rotation θ in the frequency domain, as shown in (4):

$$DFT[I(x \cos \theta - y \sin \theta, x \sin \theta + y \cos \theta)] = F(u \cos \theta - v \sin \theta, u \sin \theta + v \cos \theta). \quad (4)$$

Watermark embedding in the DFT domain has a certain number of robust properties with respect to rotation, scaling and translation (RST) invariance as well as watermark robustness against common signal processing such as JPEG compression, filtering, and noise contamination, among others. A common factor that causes watermark detection errors in invisible watermarking is the synchronization loss between the embedding and detection stages when a watermarked image is processed by geometric distortions, in this way, DFT domain is often attractive and adopted by its invariant property against RST distortions. In the last few years, several DFT-based invisible watermarking methods have been proposed in the scientific literature [6,8–17], obtaining promising results in terms of imperceptibility and robustness. When the magnitude of DFT is used as embedding domain in invisible watermarking [6,8,10,16], generally the algorithm selecting experimentally a pair of radiuses r_1 and r_2 in the magnitude $M(u,v)$ that comprises a fixed annular area $A = \pi(r_2^2 - r_1^2)$ between r_1 and r_2 that should cover the middle frequencies components in the DFT domain around the zero frequency term $M(0,0)$. The reasons are because the modifications in the lower frequencies of $M(u,v)$ will cause visible distortion in the spatial domain of the image. On the other hand, if a watermark is embedded in the higher frequencies of $M(u,v)$, the watermark is often suppressed by the JPEG compression. Thus, the watermark should be embedded in the band of the middle frequencies of $M(u,v)$ because, in this spectral region, it will be robust against common signal processing distortions, including the JPEG compression and at the same time imperceptible by naked eye. This fact is shown in Figure 1.

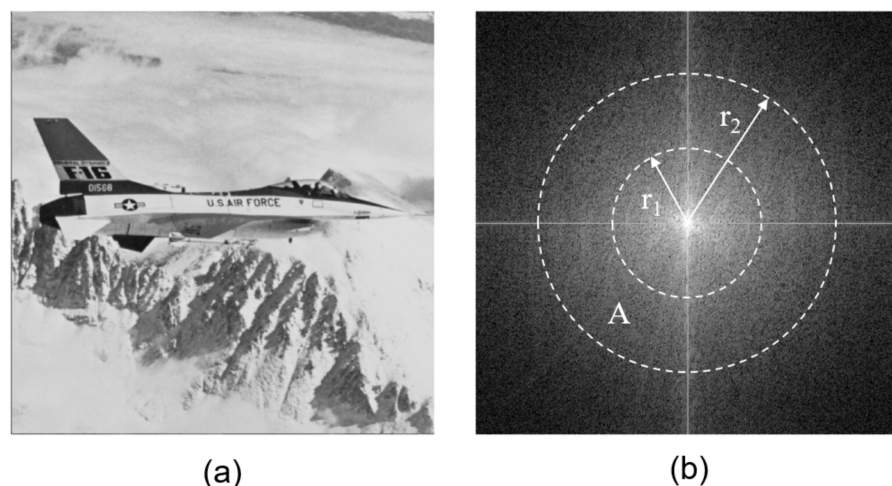


Figure 1. (a) Original image. (b) Conventional definition of embedding region in the magnitude of discrete Fourier transform (DFT) in invisible watermarking.

The conventional definition of the embedding region in Figure 1 was included for the first time in the proposal of Solachidis and Pitas in [8] and improved in subsequent years using human visual system criteria [17], hybrid domains [6,10,13], feature points [14,16], and spreading its versatility to several applications, e.g., medical imaging [11,15] or video

sequences [12]. Although the conventional definition of the embedding region in Figure 1 has a certain number of advantages in terms of imperceptibility and robustness reported in [6,8,10,16], there exists a drawback in 2D DFT-based invisible watermarking, which is detailed in the following paragraphs.

According to the application scenario and the image database, it is a common practice to adjust the key parameters. i.e., the pair of radiuses r_1 and r_2 in the magnitude $M(u,v)$ used to build the annular area A , and the watermark strength factor α , used by DFT-based invisible watermarking methods in an experimental manner. However, this manual adjustment may require exhaustive tasks and at the same time be a drawback in practical scenarios. In this way, modifying the same amount of DFT coefficients in a heterogeneous image database may be not the best choice, because, as is well known, the distribution of spectral information is not the same for all images in the dataset. For illustrative purposes, Figure 2a,b shows the DFT magnitude of the luminance of a couple of color images, the first one with predominant plain content and the second one with predominant texturized content.

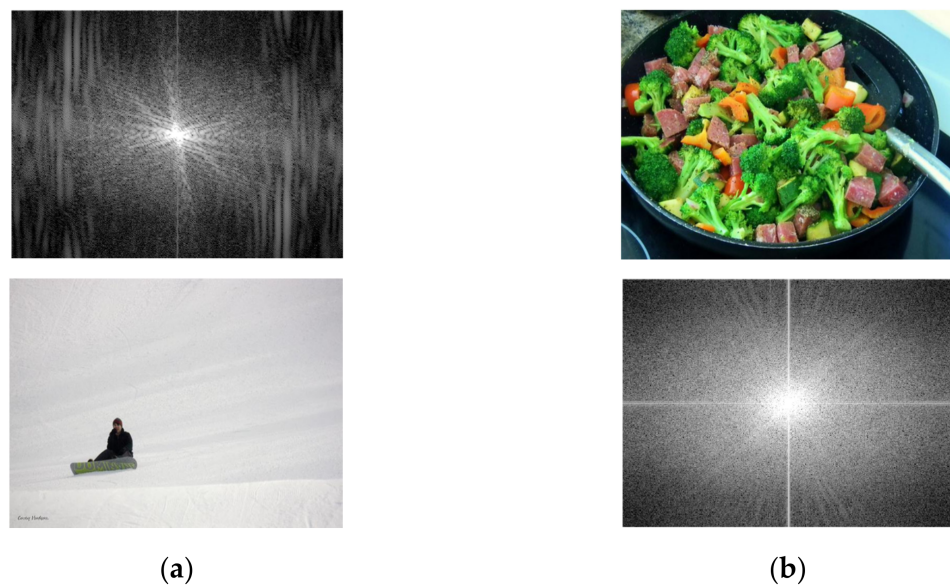


Figure 2. (a) Original image with predominant plain content and its DFT magnitude. (b) Original image with predominant texturized content and its DFT magnitude.

In this way, use of fixed values for the pair of radiuses r_1 and r_2 in the magnitude $M(u,v)$ in a heterogeneous image database, will imply that the watermark strength factor α should be adjusted experimentally in order not to affect the robustness, but invariably the watermark imperceptibility will be affected. According to the above, as shown in Figure 3, the aim of this proposal is to find the optimized values of the key parameters. i.e., the pair of radiuses r_1 and r_2 in the magnitude $M(u,v)$ used to build the annular area A , and the watermark strength factor α , proper for each image, instead to fix these values as is performed by the conventional DFT-based invisible watermarking methods, improving the performance in terms of robustness and imperceptibility using color images.

In recent years, the scientific community has focusing its attention in optimize the performance and the key parameters of invisible watermarking methods via optimization algorithms, such as PSO algorithm [5]. In this context, a brief revision of state of the art related to invisible watermarking methods that employ the PSO algorithm with optimization purposes, is shown in Table 1.

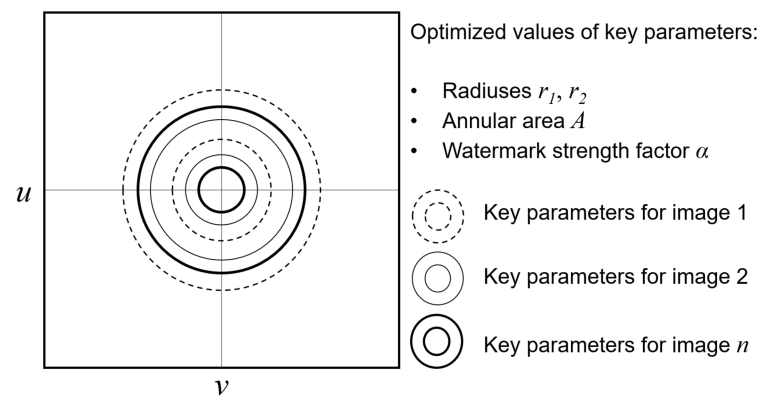


Figure 3. Aim of this proposal: find the optimized values of the key parameters in 2D DFT-based invisible watermarking.

Table 1. State of the art of invisible watermarking optimized by particle swarm optimization (PSO) algorithm.

Reference	Year	Description
[18]	2020	Robust watermarking to copyright protection based on integer wavelet transform (IWT) and guided dynamic particle swarm optimization (GDPSO).
[19]	2020	Robust blind image watermarking based on intertwining logistic map, hybrid domain using discrete cosine transform (DCT) domain, discrete wavelet transform (DWT) domain, and singular value decomposition (SVD), in conjunction with multidimensional PSO.
[20]	2020	Blind watermarking for color images based on extreme pixel adjustment (EPA), multi-bit partly sign-altered mean modulation (MP-SAM), mixed modulation (MM), quaternion discrete Fourier transform (QDFT), and PSO.
[21]	2021	Image watermarking scheme based on DWT and SVD using human visual system (HVS) and PSO.
[22]	2019	Digital watermarking algorithm with dual embedding in DCT-DWT-SVD domains, using PSO.
[23]	2019	Image watermarking using normalized block processing (NBP), normalized singular value decomposition (NSVD), IWT, DCT, a genetic algorithm (GA) and PSO.
[24]	2019	Digital image watermarking based on SVD in complex wavelet transform (CWT) domain, employing PSO and Jaya algorithm.
[25]	2019	Robust image watermarking performed in multiple transforms Lifting wavelet transform (LWT), DCT, discrete fractional angular transform (DFAT), SVD, and PSO.
[26]	2018	Robust image watermarking based on hybrid domain composed by LWT-DCT-SVD and using PSO.
[27]	2018	Digital image watermarking for industry applications in DWT-SVD domain and employing GDPSO algorithm.
[28]	2018	Image watermarking with criteria of region of interest (ROI) and region of non-interest (RONI), based on DWT-DCT-SVD domain and using PSO algorithm.

Table 1 shows a current trend in the scientific community related to the use of PSO algorithm to improve the performance of invisible watermarking based on several frequency

domains. In this way, motivated by this trend as well as by the promissory results in terms of imperceptibility and robustness obtained until now by the 2D DFT-based invisible watermarking; and justified by the necessity of improving aspects of information security related to ownership authentication and copyright protection, in this paper we propose a new improved 2D DFT-based invisible watermarking by the PSO algorithm, which is applied to color images.

The main contributions of the proposed improved 2D DFT-based invisible watermarking by the PSO algorithm are:

- Instead of using the metrics peak signal to noise ratio (PSNR)/structural similarity index (SSIM) in the fitness function of PSO algorithm, we employ the metric visual information fidelity (VIF) in conjunction with BCR criterion. It is known in the literature [29] that the VIF value reflects perceptual distortions more precisely than the PSNR. The range of VIF values is [0, 1], where the closer value to 1 represents the better fidelity with respect to the original image;
- To improve the robustness, we consider a set of geometric and signal processing attacks in the fitness function of the PSO algorithm, each one with aggressive image distortion;
- Instead of performing the imperceptibility and robustness testing using the classic images such as Lena, Baboon, etc., the proposed method is tested on 1000 color images extracted from COCO dataset [30], which contains images of complex everyday scenes with common objects in their natural context;
- Imperceptibility testing is performed using PSNR and VIF metrics;
- Robustness testing is performed considering a wide range of geometric, common signal processing and combined distortions;
- Detailed performance comparison with the conventional 2D DFT-based invisible watermarking is performed to show the improvements in terms of imperceptibility and robustness when the PSO optimization is adopted.

3. Proposed Method

This section presents the embedding and extraction stages of the watermark, as well as the optimization procedure based on PSO.

3.1. Embedding Process

According to [31,32], the red-green-blue (RGB) color model has the most correlated components, the YCbCr has the least correlated and the forward and backward transformations between both color models are linear; in this way, considering a color image I :

1. Perform RGB-YCbCr color model transformation and isolates the luminance component $Y(x,y)$ from YCbCr transformation;
2. Supported by a secret key k_1 , generate a watermark which is a 1-D binary $\{1, 0\}$ pseudo-random pattern with zero mean, $W = \{w_b \mid b = 1, \dots, L\}$, where L is the length of the watermark;
3. Apply the 2D DFT transform $F(u,v)$ defined by (1) to the original luminance component $Y(x,y)$ and obtain the magnitude $M(u,v)$ and phase $P(u,v)$ information;
4. Select a pair of radiuses r_1 and r_2 in $M(u,v)$ and the annular area $A = \pi(r_2^2 - r_1^2)$ between r_1 and r_2 should cover the middle frequency in $M(u,v)$ around the zero frequency coefficient $M(0,0)$;
5. To guarantee the security of W , scramble its data bits using a secret key k_2 ;
6. Encode W using the spread spectrum modulation DS-CDMA: with a predefined secret key k_3 , assign to each watermark data bit w_b a pseudorandom binary $\{-1, 1\}$ sequence g_b with length $A/2$. Each g_b sequence is dependent on w_b in the following way:

$$\begin{aligned} \text{if } w_b = 0 &\rightarrow +g_b \\ \text{if } w_b = 1 &\rightarrow -g_b \end{aligned} \quad (5)$$

The encoded watermark $W_{DS-CDMA}$ is obtained using (6):

$$W_{DS-CDMA} = \sum_{b=1}^L \pm g_b \quad (6)$$

1. Embed the encoded watermark $W_{DS-CDMA}$ in the coefficients of the upper half of $M(u,v)$ in the annular area $A/2$ that cover the middle frequency, in an additive manner:

$$M'(u,v) = M(u,v) + \alpha W_{DS-CDMA} \quad (7)$$

where α is the watermark strength factor and M, M' , are the original and the watermarked DFT magnitude, respectively. According to DFT symmetrical properties, to produce real values after the watermark embedding, the lower half part of the middle frequency band of $M(u,v)$ should be modified symmetrically.

2. Return the watermarked luminance component $Y'(x,y)$ to spatial domain using the inverse DFT (IDFT) employing $M'(u,v)$ and the corresponding initial phase $P(u,v)$ as shown in (8):

$$\begin{aligned} Y'(x,y) &= IDFT(F'(u,v)), \text{ where :} \\ F'(u,v) &= M'(u,v) \cdot \cos(P(u,v)) + M'(u,v) \cdot (j \cdot \sin(P(u,v))); \end{aligned} \quad (8)$$

3. Finally, using the watermarked luminance $Y'(x,y)$ and the original chrominance information, perform YCbCr to RGB color model transformation and obtain the watermarked image I_w .

3.2. Extraction Process

The extraction process is described as follows:

1. Considering the color watermarked image I_w , perform RGB-YCbCr color model transformation and obtain the watermarked luminance $Y'(x,y)$;
2. Compute the 2D DFT transform $F'(u,v)$ from $Y'(x,y)$ and get the watermarked magnitude $M'(u,v)$;
3. The annular area A is computed employing the values of radiuses r_1 and r_2 used in the embedding process;
4. Split $M'(u,v)$ in two parts, the upper half, and the lower half respectively;
5. By symmetrical DFT properties, considering only the information from the upper half part of $M'(u,v)$, the embedded watermark can be extracted using the secret key k_3 , computing the linear correlation c_b between the normalized watermarked magnitude coefficients M' normalized and b -th pseudorandom pattern g_b as follows:

$$c_b = \sum_{b=1}^L ((g_b - \hat{g}_b) \cdot M'_{normalized}), \quad (9)$$

where \hat{g}_b is the average of all values in g_b and $M'_{normalized} = M' - M'_{av}$, where M'_{av} is the average of all values in $M'(u,v)$;

6. Recover the watermark data bits of $W' = \{w'_b \mid b = 1, \dots, L\}$ using the sign function as follows:

$$\text{if } \text{sign}(c_b) \text{ is "+" then } w'_b = 0, \text{ otherwise } w'_b = 1; \quad (10)$$

7. Finally, rearrange W' using the secret key k_2 .

4. Optimization Key Parameters by Particle Swarm Optimization (PSO)

The PSO algorithm was first introduced by [5] in 1995. In general terms, PSO is a search and optimization method for swarm intelligence techniques and evolutionary algorithms. According to [5], the PSO algorithm is inspired by the social behavior of a group of individuals (in PSO denoted as a particle) e.g., as a flock of birds moving together. Each particle keeps track of the individual best value, and PSO searches the global best

solution in terms of the objective fitness function [19]. PSO is defined as updating velocity v of each particle (11) and updating position δ of each particle (12), respectively:

$$v_{i,j}(t + 1) = \omega \cdot v_{i,j}(t) + \underbrace{rand()C_1(p_{i,j}(t) - \delta_{i,j}(t))}_{\text{Cognitive component}} + \underbrace{rand()C_2(\eta_j(t) - \delta_{i,j}(t))}_{\text{Social component}}, \quad (11)$$

$$\delta_{i,j}(t + 1) = \delta_{i,j}(t) + v_{i,j}(t + 1). \quad (12)$$

From (11) and (12):

- Subscript i denotes the particle index $1 \leq i \leq$ population size N ;
- Subscript j denotes the dimension of feature space index;
- ω is the inertia coefficient;
- C_1 is the personal speedup coefficient;
- C_2 is the social speedup coefficient;
- $rand()$ is a pseudo-random number generator (PRNG) with uniform distribution in the range $[0, 1]$;
- t denotes time;
- $p_{i,j}(t)$ is the position that provides the minimum cost of the j -th element of the i -th particle;
- $\eta_j(t)$ is the position that provides the minimum cost of all existent particles.

In the sake of brevity, interested readers on initialization, the search of best solution, iteration and convergency procedures of PSO, can refer to [5,19] for more details. As was mentioned in Section 2, use of fixed values for the pair of radiuses r_1 and r_2 in the magnitude $M(u,v)$ in a heterogeneous image database will imply that the watermark strength factor α will be adjusted experimentally so as not to affect the robustness, but invariably the watermark imperceptibility will be affected. Thus, the aim of this proposal is to find the optimized values of the key parameters i.e., the pair of radiuses r_1 and r_2 in the magnitude $M(u,v)$ used to build the annular area A , and the watermark strength factor α , proper for each image, instead to fix these values as is performed by the conventional DFT-based invisible watermarking methods, improving the performance in terms of robustness and imperceptibility using color images. The optimization procedure of watermarking parameters based on PSO is shown in Figure 4.

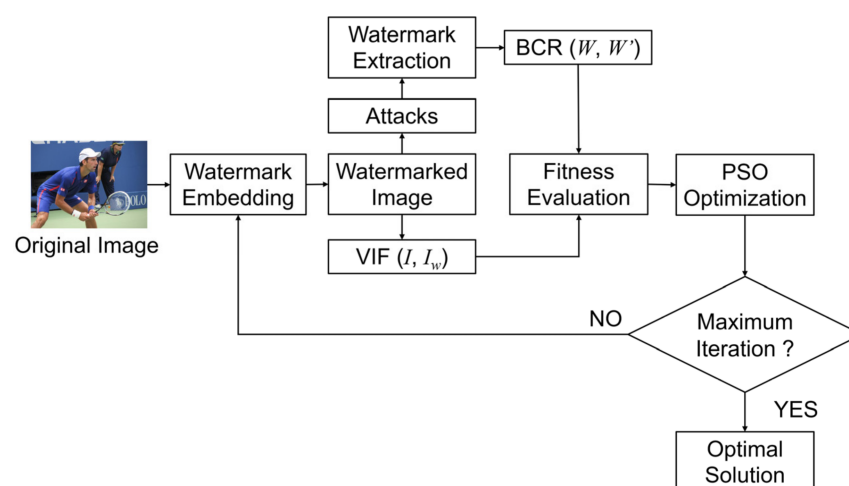


Figure 4. Optimization process of the key parameters in 2D DFT-based invisible watermarking using PSO.

In PSO algorithm, the fitness value of each particle is assessed in each iteration. An objective fitness function for evaluation should reflect both imperceptibility and robustness. In this proposal, the fitness function is given by (13):

$$f = VIF(I, I_w) + \frac{\sum_{q=1}^n BCR(W, W'_q)}{n}, \tag{13}$$

where f represents the fitness value in each iteration. The VIF metric [29] measures the imperceptibility between the original image I and its watermarked version I_w , BCR estimates the robustness, W and W' are the original and extracted watermarks respectively, and n is the number of attacks applied to the watermarked images. The VIF metric is defined by (14) as:

$$VIF = \frac{\sum_{k \in channels} I(\overset{\rightarrow Z,k}{C}; \overset{\rightarrow Z,k}{G} | s^{Z,k})}{\sum_{k \in channels} I(\overset{\rightarrow Z,k}{C}; \overset{\rightarrow Z,k}{E} | s^{Z,k})}, \tag{14}$$

where we sum the channels of interest, $\overset{\rightarrow Z,k}{C}$ represents Z elements of the random field (RF), C_k describes the coefficients from channel k , and so on [29]. E and G denote the visual signal at the output of the HVS model from the original and watermarked images respectively, from which the brain extracts cognitive information.

The terms $I(\overset{\rightarrow Z,k}{C}; \overset{\rightarrow Z,k}{E} | s^{Z,k})$ and $I(\overset{\rightarrow Z,k}{C}; \overset{\rightarrow Z,k}{G} | s^{Z,k})$ represent the mutual information that can ideally be extracted by the brain from a particular channel in the original and the watermarked images, respectively, given a reference image [29]. As is known in the literature, the VIF value reflects perceptual distortions more precisely than peak signal to noise ratio (PSNR). The range of VIF is $[0, 1]$ where the closer value to 1 represents the better fidelity with respect to the original image. On the other hand, BCR is defined by (15) as:

$$BCR = \frac{L - \sum_{b=1}^L W_b \oplus W'_b}{L} \tag{15}$$

where W and W' are the original and extracted watermarks respectively, L is the watermark length and \oplus denotes a module 2 addition, or XOR operation. In this paper, we employ five attacks ($n = 5$) in (13). These signal processing and geometric distortions are shown in Table 2.

Table 2. Signal processing and geometric distortions considered in the fitness function of the PSO algorithm.

Distortion	Tolerance
Centered cropping	100 × 100 for images with spatial resolution of 640 × 480
Box filter	Kernel of 5 × 5
Downsizing	Scaling factor of 0.6
JPEG compression	Quality factor 30
Gaussian noise	$\mu = 0, \sigma^2 = 0.01$

The fitness value increases when VIF and BCR values grow. The VIF [29] and BCR values have been multiplied by 100, since its normal values fall in the range $[0, 1]$. In training of the PSO algorithm, the watermark strength factor $\alpha \in [0.5 - 10.5]$ and the pair of radiuses r_1 and r_2 in the magnitude $M(u,v)$ are $r_1 \in [10 - 100]$ and $r_2 \in [105 - 250]$. The parameter values in the PSO algorithm are given in Table 3.

Table 3. Parameter setting of PSO algorithm.

Maximum Number of Iterations	Population Size N	Cognitive and Social Factors C_1, C_2	Inertia Coefficient ω
100	10	2.0	1.0–0.99

5. Experimental Results and Discussion

This section presents the experimental results for this proposal. The proposed method was tested on 1000 color images extracted from the COCO dataset [30], which contains images of complex everyday scenes with common objects in their natural context. The experimentation was performed in terms of imperceptibility and robustness. To provide clarity in the testing, the results are reported as “PSO-DFT” and “Conventional DFT” labels in each figure, to show the improvements of performance obtained using the PSO algorithm in 2D DFT-based invisible watermarking. For conventional 2D DFT-based invisible watermarking, the values of pair of radiuses r_1 and r_2 are fixed at 50 and 150, respectively, and the value of the watermark strength α is 1.5, accordingly to our previous proposal reported in [6].

5.1. Watermark Imperceptibility

Considering 1000 color images extracted from COCO dataset [30], and a binary watermark of $L = 32$ bits, in Figures 5 and 6 we summarize the PSNR and VIF obtained for each image in the dataset.

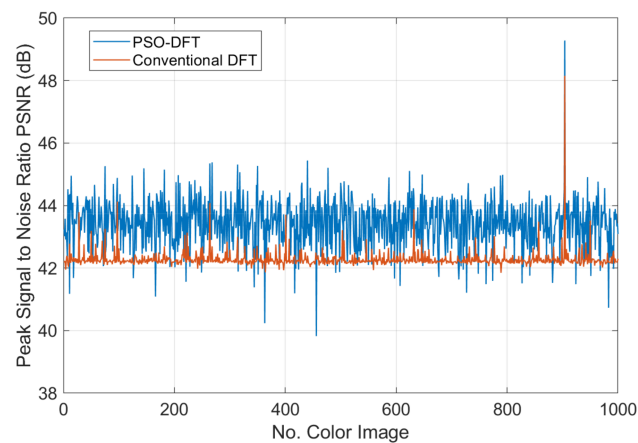


Figure 5. Peak signal to noise ratio (PSNR) of 1000 images from COCO dataset employing (blue plot) and non-employing (orange plot) PSO algorithm.

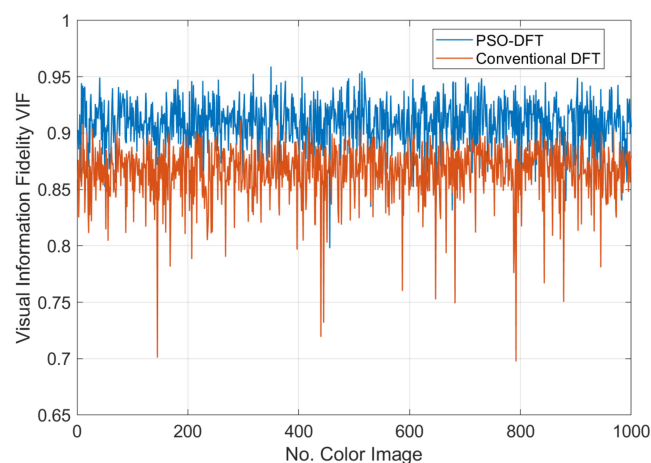


Figure 6. Visual information fidelity (VIF) of 1000 images from COCO dataset employing (blue plot) and non-employing (orange plot) PSO algorithm.

From Figure 5 we show that the average PSNR obtained employing PSO is 43.42 dB, meanwhile, not using PSO it is 42.27 dB. In terms of average PSNR the gain in dB is hardly 1.15 dB. However, there exist two aspects that must be considered: The first one is that, from

Figure 5 the comparative one-to-one show in almost all images a gain of approximately 1.5–2 dB, meanwhile for few images there is a small loss in dB. This behavior is related to the trade-off between imperceptibility-robustness of digital watermarking. The second one, and the most relevant, as is known in the literature, is that the VIF value reflects perceptual distortions more precisely than peak signal to noise ratio (PSNR) according to reference [29]. The range of VIF is [0, 1] where the closer value to 1 represents the better fidelity respect to the original image. In this way, the imperceptibility results in terms of VIF are shown in Figure 6.

From Figure 6 we show that the average VIF obtained employing PSO is 0.9086 meanwhile not using PSO it is 0.8659. In terms of average VIF the gain is hardly of 0.0427. The comparative one-to-one show in almost all images is a gain of approximately 0.05–0.08, meanwhile for a few images there is a small loss in VIF value. Again, this is a trade-off between the imperceptibility and robustness of digital watermarking. With illustrative purposes, Figure 7 shows a resultant image employing and non-employing PSO algorithm, considering a binary watermark of $L = 64$ bits.

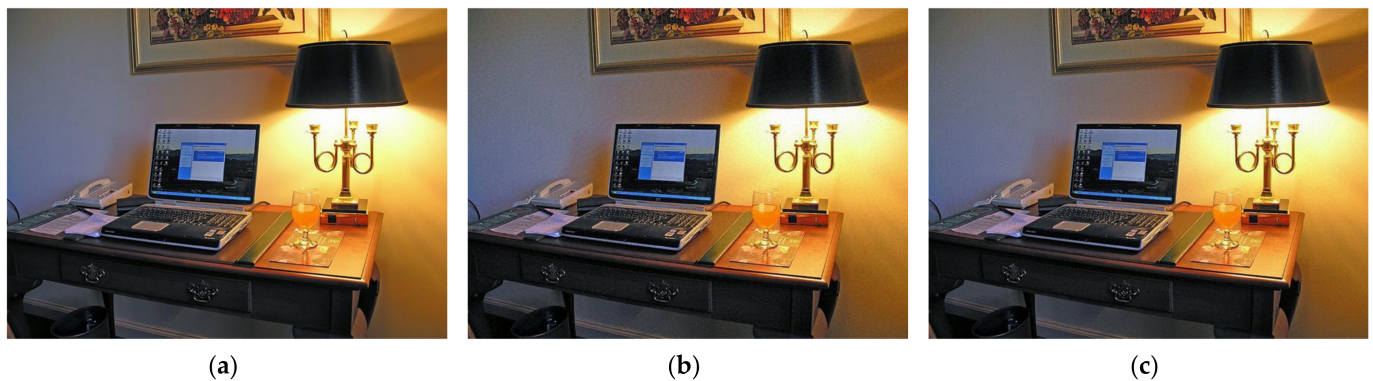


Figure 7. (a) Original image. (b) Watermarked image using conventional discrete Fourier transform (DFT), $r_1 = 50$, $r_2 = 150$, $\alpha = 1.5$, $L = 64$, PSNR = 39.65 dB, VIF = 0.78. (c) Watermarked image using PSO-DFT, $r_1 = 79$, $r_2 = 250$, $\alpha = 0.5$, $L = 64$, PSNR = 42.07 dB, VIF = 0.86.

As mentioned above, we show that although in quantitative form the imperceptibility results using PSO outperform slightly conventional DFT, the visual quality regarding to the original image is remained when the PSO is employed, as shown in Figure 7. The major benefit in terms of visual quality is obtained in flat regions, where usually the 2D DFT-based invisible watermarking causes a noise effect, as shown in Figure 7.

Considering a watermark length $L = 32$, the optimized values using PSO algorithm for the pair of radiuses r_1 and r_2 , as well as for the value of the watermark strength α ; and the PSNR and VIF values obtained by PSO-DFT and conventional DFT watermarking are shown in Table 4. Additionally, for illustrative purposes, the PSO convergence history of the proposed method for a couple of images are shown in Figures 8 and 9 respectively. Figure 10 shows PSO convergence of 50 images from the COCO dataset.



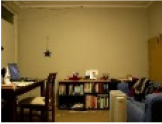


5.2. Watermark Robustness

To evaluate the watermark robustness of the proposed method, we used several signal processing, geometrical attacks, and combined attacks. Assuming ergodicity, the BCR is defined as the ratio between the number of correctly decoded bits and the total number of embedded bits. According to [6,33], a threshold value Th must be defined to determine the presence or absence of the watermark W . To formalize the computation of Th , we consider a binomial distribution with success probability equal to 0.5, and then the false alarm probability P_{fa} for L bits is given by (16), and a threshold value T in (16) must be provided to P_{fa} becomes smaller than a predetermined value [6,33].

$$P_{fa} = \sum_{z=T}^L (0.5)^L \cdot \left(\frac{L!}{z!(L-z)!} \right) \tag{16}$$

where L is the watermark length. Based on the Bernoulli trials assumption, z is independent random variable with binomial distribution [33]. In this way, considering $L = 32$ and $T = 25$, the $P_{fa} = 0.0011$ and $Th = T/L = 25/32 = 0.78$. Recall by the inclusion-exclusion probability principle that the addition of the bit error rate (BER) and BCR must equal 1. Note that the values of T , P_{fa} and Th are adjusted according to the value assigned to the watermark length L .

Table 4. Performance comparison in terms of PSNR and VIF between the optimized values of r_1 , r_2 and α using PSO algorithm vs. fixed values in conventional DFT watermarking.

Image	PSO-DFT					Conventional DFT				
	r_1	r_2	α	PSNR (dB)	VIF	r_1	r_2	α	PSNR (dB)	VIF
	86	110	2.62	43.17	0.90				42.14	0.87
	61	143	0.65	44.96	0.94				42.33	0.81
	71	105	1.97	43.82	0.92	50	150	1.5	42.21	0.87
	56	153	0.67	44.70	0.93				42.26	0.83
	76	108	1.51	44.30	0.95				42.24	0.88

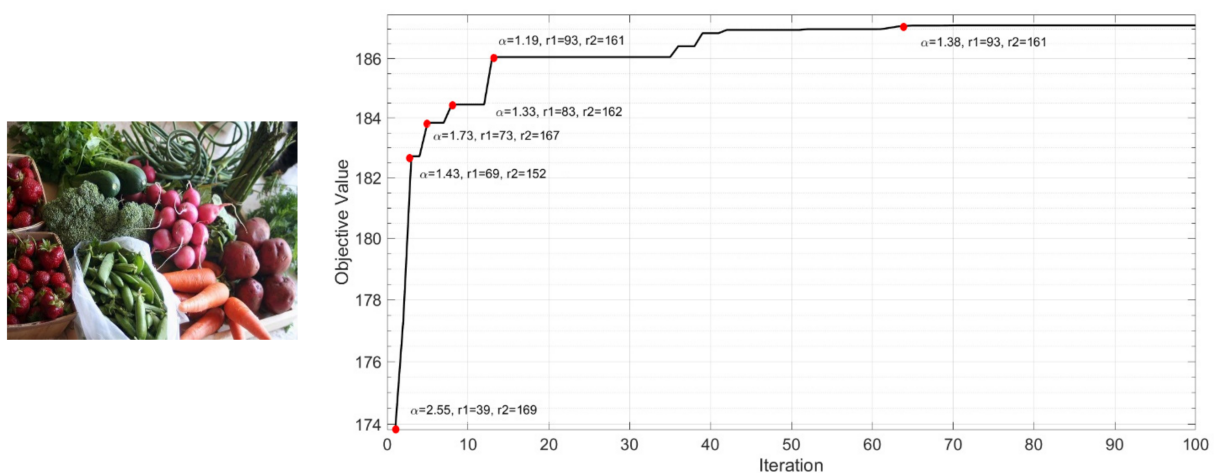


Figure 8. The PSO convergence history of the proposed method using an image with predominant texturized content.

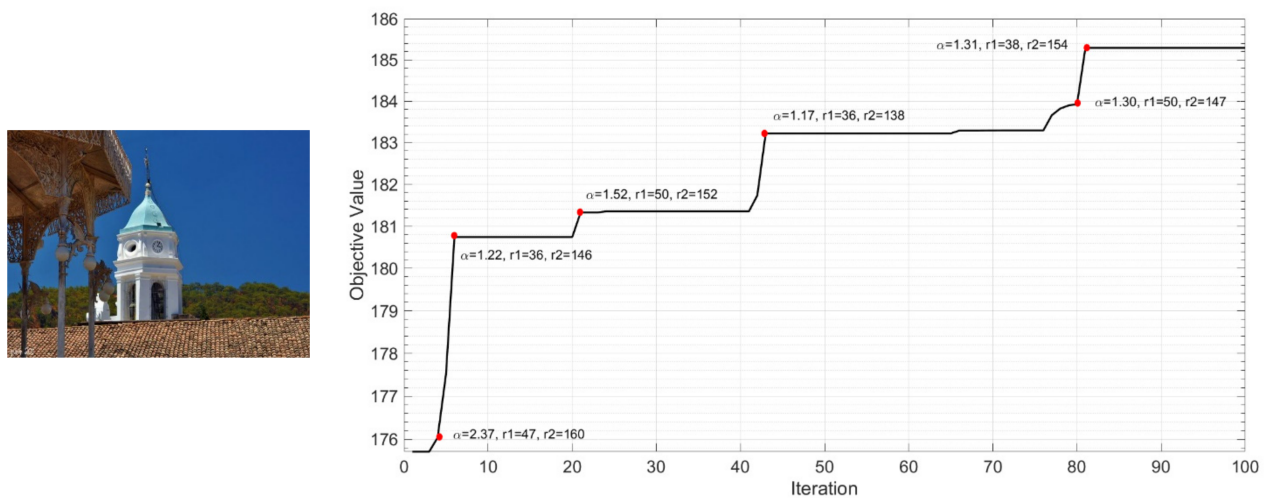


Figure 9. The PSO convergence history of the proposed method using an image with predominantly plain content.

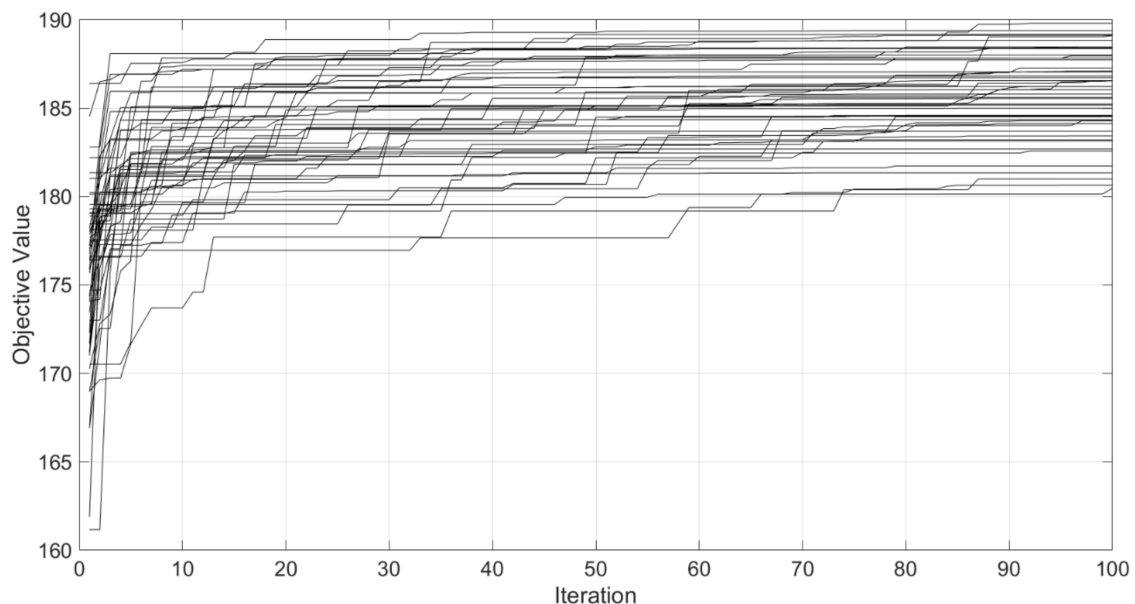


Figure 10. The PSO convergence of 50 images from the COCO dataset.

5.2.1. Signal Processing Distortions

Considering 1000 color images extracted from the COCO dataset [30], and a binary watermark of $L = 32$ bits, in Figure 11 we summarize the average BCR obtained by PSO-DFT and conventional DFT watermarking respectively, against the several signal processing distortions, such as Joint Photographic Experts Group (JPEG) compression, among others, given in Table 5. The values of a pair of radiuses r_1 and r_2 are fixed at 50 and 150, respectively, and the value of the watermark strength α is 1.5, according to the conventional proposal previously reported in [6]. For the sake of brevity, in this testing we include aggressive tolerances for some attacks, assuming that the minor tolerances are detected in a successful manner.

As shown in Figure 11, the optimized 2D DFT-based watermarking by PSO algorithm outperforms to the conventional 2D DFT image watermarking in terms of watermark robustness against several signal processing. The relevant improvements are when the watermarked image is distorted by the attacks in Table 6. Italics in Table 6 indicate that the detection has failed.

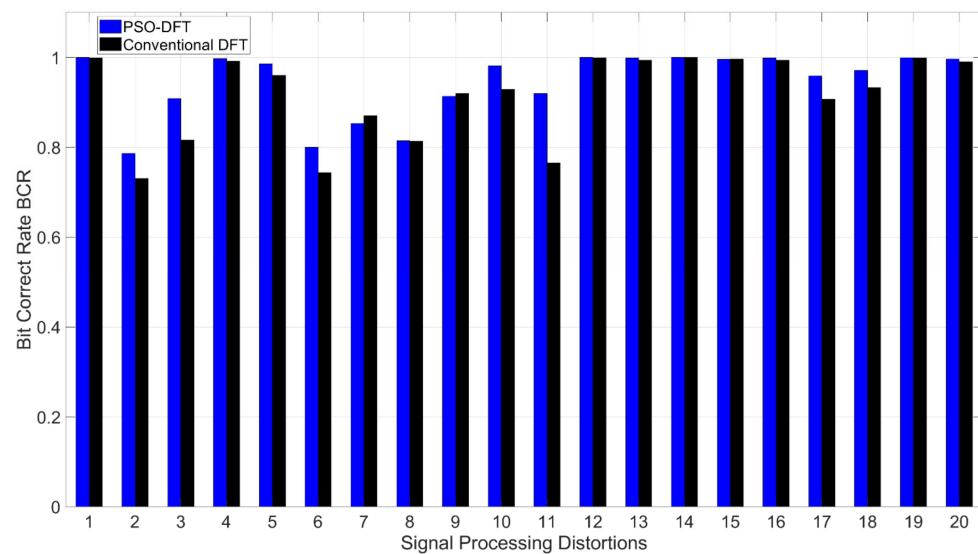


Figure 11. Average bit correct rate (BCR) against signal processing distortions.

Table 5. Summary of signal processing distortions applied to watermarked images.

ID: Signal Processing Distortion	
1: Without distortion	11: Box filter 5×5
2: JPEG lossy compression QF = 20	12: Histogram equalization
3: JPEG lossy compression QF = 30	13: Gaussian filter 7×7
4: JPEG lossy compression QF = 50	14: Sharpening
5: Gaussian noise $\mu = 0$ and $\sigma^2 = 0.01$	15: Brightness increase
6: Gaussian noise $\mu = 0$ and $\sigma^2 = 0.05$	16: Brightness reduction
7: Impulsive noise density = 0.09	17: Median filter 3×3
8: Speckle noise $\mu = 0$ and $\sigma^2 = 0.2$	18: Motion filter 5×5
9: Speckle noise $\mu = 0$ and $\sigma^2 = 0.09$	19: Gamma correction $\gamma = 2$
10: Box Filter 3×3	20: Gamma correction $\gamma = 0.5$

Table 6. Relevant improvements obtained by PSO-DFT in terms of average BCR against signal processing distortions.

Signal Processing Distortion	Average BCR PSO-DFT	Average BCR Conventional DFT
JPEG lossy compression QF = 20	0.79	0.73
JPEG lossy compression QF = 30	0.90	0.81
Gaussian noise $\mu = 0$ and $\sigma^2 = 0.05$	0.80	0.74
Box Filter 3×3	0.98	0.92
Box filter 5×5	0.92	0.76
Median filter 3×3	0.96	0.90
Motion filter 5×5	0.97	0.93

From Figure 11, we show that against the signal processing distortions described in Table 5, the PSO-DFT watermarking keep the robustness obtained by the conventional 2D DFT watermarking, obtaining average BCR values over the threshold value $Th = 0.78$.

5.2.2. Combined Distortions: JPEG Quality Factor (QF) = 70 + Signal Processing Distortions

Considering 1000 color images extracted from the COCO dataset [30], and a binary watermark of $L = 32$ bits, in Figure 12 we summarize the average BCR obtained by PSO-DFT and conventional DFT watermarking respectively, against combined distortions composed by JPEG compression with quality factor 70+ several signal processing distortions given in Table 7.

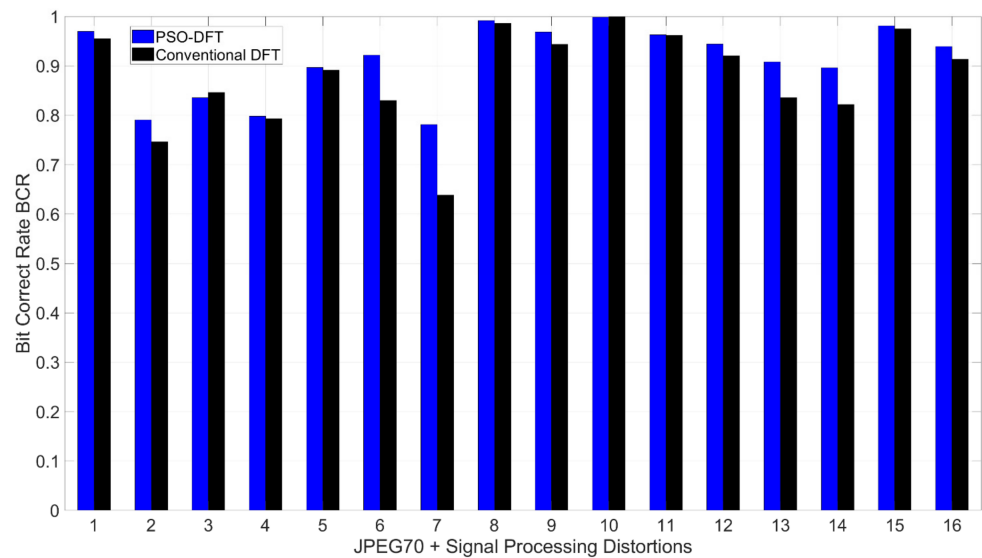


Figure 12. Average BCR against combined attacks composed by JPEG QF = 70 + signal processing distortions.

Table 7. Summary of combined attacks composed by JPEG QF = 70 + signal processing distortions applied to watermarked images.

ID: JPEG70 + Signal Processing Distortion	
1: Gaussian noise $\mu = 0$ and $\sigma^2 = 0.01$	9: Gaussian filter 7×7
2: Gaussian noise $\mu = 0$ and $\sigma^2 = 0.05$	10: Sharpening
3: Impulsive noise density = 0.09	11: Brightness increase
4: Speckle noise $\mu = 0$ and $\sigma^2 = 0.2$	12: Brightness reduction
5: Speckle noise $\mu = 0$ and $\sigma^2 = 0.09$	13: Median filter 3×3
6: Box Filter 3×3	14: Motion filter 5×5
7: Box filter 5×5	15: Gamma correction $\gamma = 2$
8: Histogram equalization	16: Gamma correction $\gamma = 0.5$

As shown in Figure 12, the optimized 2D DFT-based watermarking by PSO algorithm outperforms the conventional 2D DFT image watermarking in terms of watermark robustness against several combined distortions in Table 7. The relevant improvements are when the watermarked image is distorted by the combined attacks in Table 8. Italics in Table 8 indicate that the detection has failed.

Table 8. Relevant improvements obtained by PSO-DFT in terms of average BCR against the combination of JPEG quality factor (QF) = 70 + signal processing distortions.

JPEG QF = 70+	Average BCR PSO-DFT	Average BCR Conventional DFT
Gaussian noise $\mu = 0$ and $\sigma^2 = 0.05$	0.79	<i>0.74</i>
Box Filter 3×3	0.92	0.82
Box Filter 5×5	0.79	<i>0.63</i>
Median filter 3×3	0.90	0.83
Motion filter 5×5	0.89	0.82

From Figure 12 we show that against the rest of combined distortions in Table 7, the PSO-DFT watermarking keeping the robustness obtained by the conventional 2D DFT watermarking, obtaining average BCR values over the threshold value $Th = 0.78$.

5.2.3. Geometric Distortions and Combined Attacks

Considering 1000 color images extracted from the COCO dataset [30], and a binary watermark of $L = 32$ bits, in Table 9 we summarize the average BCR obtained by PSO-DFT and conventional DFT watermarking, respectively, against geometric manipulations and combined attacks composed by JPEG compression with quality factor 70+ geometric distortions. Italics in Table 9 indicate that the detection has failed. For the sake of brevity, in this test we included aggressive tolerances assuming that the minor tolerances are detected in a successful manner. From Table 9, we show that the optimized 2D DFT-based watermarking by PSO algorithm outperforms to the conventional 2D DFT image watermarking in terms of watermark robustness against attacks that involve image resizing by scaling factor 0.6, as well as random cropping by 35% combined with re-scaling and JPEG compression with QF = 70. To the rest of geometric manipulations, the PSO-DFT watermarking keeping the robustness obtained by the conventional 2D DFT watermarking, obtaining average BCR values over the threshold value $Th = 0.78$. This behavior is due to the fact that the watermark embedding in the DFT domain has a certain number of robust properties with respect to rotation, scaling and translation (RST) invariance. The robustness against general affine transformation is supported by our resynchronization method previously reported in the literature. For more details of the resynchronization technique, interested readers can refer to [16].

Table 9. Average BCR against geometric manipulations and combined attacks composed by JPEG QF = 70 + geometric distortions.

Distortion	Average BCR PSO-DFT	Average BCR Conventional DFT
Rotation by 45° with auto-crop	0.98	0.96
Rotation by 135° with auto-crop	0.97	0.92
Resizing, scaling factor = 0.6	0.96	0.77
Resizing, scaling factor = 2	0.99	0.99
Central cropping 120 × 120	0.98	0.97
Translation $x = 100, y = 100$	0.96	0.96
Affine [0.9,0.2,0;0.1,1.2,0;0,0,1]	0.99	0.98
Shearing (0, 20%)	0.99	0.99
Aspect Ratio (1.0, 1.2)	0.99	0.97
Aspect Ratio (0.8, 1.0)	0.99	0.98
JPEG70 + Rotation by 55° with auto-crop	0.90	0.87
JPEG70 + Rotation by 115° with auto-crop	0.89	0.85
JPEG70 + Resizing, scaling factor = 0.6	0.92	0.76
JPEG70 + Resizing, scaling factor = 2	0.95	0.93
JPEG70 + cropping 35% with re-scaling	0.81	0.76
JPEG70 + Translation $x = 100, y = 100$	0.87	0.85
JPEG70 + Affine [0.9,0.2,0;0.1,1.2,0;0,0,1]	0.97	0.96
JPEG70 + Shearing (20%, 0)	0.96	0.96
JPEG70 + Aspect Ratio (1.0, 1.2)	0.97	0.95
JPEG70 + Aspect Ratio (0.8, 1.0)	0.98	0.98

5.3. Analysis and Discussion

From the experimental results shown in Sections 5.1 and 5.2 which are performed in terms of imperceptibility and robustness, respectively, we view several benefits in the use of PSO algorithm to optimize the 2D DFT-based watermarking that employs spread spectrum modulation DS-CDMA.

The first one is related to the use of the VIF metric in the fitness function of PSO, because as is known in the literature, the VIF value reflects perceptual distortions more precisely than PSNR. The major benefit in terms of visual quality is obtained in flat regions of digital images, where usually the conventional DFT-based watermarking causes a noise effect by considering a fixed value of watermark strength and the middle frequency bands in the magnitude of DFT to all images in a dataset. In this research a priori we known the fix

values of a pair of radiuses r_1, r_2 , and the watermark strength α , based on our conventional DFT-based proposal reported in [6], all obtained in an experimental form.

The second one is related to the five attacks used in the fitness function of PSO: centered cropping of 100×100 for images with spatial resolution of 640×480 , a box filter with kernel of 5×5 , downsizing using scaling factor of 0.6, JPEG compression with quality factor = 30, and Gaussian noise with $\mu = 0$ and $\sigma^2 = 0.01$. From experimental results in Section 5.2 we show the benefits of the use of the PSO algorithm in terms of robustness against JPEG lossy compression with a quality factor (QF) less than 30, Gaussian noise contamination, several filtering operations including mean, median and motion filters, cropping and downsizing as well as combined distortions, keeping the good robustness obtained by the conventional 2D DFT watermarking in the rest of the attacks, and confirming that the five attacks included in the fitness function of PSO are sufficient to improve the performance of the conventional 2D DFT watermarking, which in its original form is weak against these five attacks.

The third one is related to the watermark security. In invisible watermarking, imperceptibility and robustness are not the only constraints to deal with but the security is important too. Considering the pair of radiuses r_1, r_2 , as a secret key of a given 2D DFT-based image watermarking, the use of the same secret key for marking a lot of images may be is not the best choice, because is possible for an adversary to estimate the secret key if he owns more than one watermarked content [34]. Estimation of the secret key can be very dangerous, especially for image content: if the database of images is stolen, the adversary would be able to infringe the copyright and intellectual property, so watermarking needs to be handled with care. In this way, when setting the fixed values for the secret key (pair of radiuses r_1, r_2), the security of the conventional DFT-based watermarking is very compromised. To solve this security issue, the PSO algorithm has a fundamental role, finding the unique secret key to each image in a given dataset, moreover providing benefits in imperceptibility and robustness.

Finally, Table 10 shows a comparison performance by considering the previously reported methods in [19–26] and our proposal. A grid cell appears with a dash '-', when the authors did not report a criterion or simulation. Comparatively, we consider only relevant criteria, as they are the most essential in the design of a robust digital watermarking optimized by the PSO algorithm.

For the sake of brevity, we perform a punctual comparison in Table 10. Is clear that our proposed method is outperformed by all the works in Table 10 in terms of watermark payload, because in all of them the purpose is prioritize the capacity of watermarking techniques. However, although the capacity is relatively high, there exist several drawbacks by the current state-of-the-art. One of them is related to the weakness against geometric distortions, focusing its attention only on the rotation, cropping and resizing. There exist more geometric distortions that need to be considered in the design of a robust watermarking. A trend in the current state-of-the-art is the use of PSNR as the imperceptibility metric in the fitness function of PSO. The benefits of the use of VIF instead of PSNR are clear, as shown along the experimental results in this paper. Future research in the scientific literature may consider another imperceptibility metrics different to PSNR in the fitness function of PSO, to obtain improvements in terms of the image quality of the watermarked images. Another important aspect is the number of images used in the experimental results as well as its bit depth resolution. In this sense, in Table 10 we show that almost all works in the current state-of-the-art [19,21,22,24–26] performed experiments on a few digital images (less than 10 images) with 8-bit grayscale resolution, to exception of the work in [20] which consider 64 color images with 24 bit/pixel of resolution. However, considering a few images in a watermarking test may be a drawback for implementing the watermarking algorithm in large scale image datasets. In this way, massive testing in terms of imperceptibility and robustness considering large image datasets should be compulsory, as the case of our proposal that considers a dataset of 1000 color images with 24 bit/pixel of

resolution. Finally, all proposals in Table 10 are competitive in terms of robustness against JPEG compression and noise image corruption.

Table 10. Performance comparison.

Method	JPEG Compression	Watermark Payload	Imperceptibility Metric Used in PSO Fitness Function	Detection Metric Used in PSO Fitness Function	Maximum Number of Iterations in PSO	Number of Images in Trials/Bit Depth	Geometric Attacks	Types of Noises
[19]	10–100	1024 bits	PSNR	BER	30	8 images in grayscale with 8 bit/pixel in depth	Resizing, Cropping	Gaussian, Salt and pepper, Speckle
[20]	20–100	4096 bits	PSNR-Mean SSIM	BER	30	64 images in color with 24 bit/pixel in depth	Cropping	Gaussian, Salt and pepper, Speckle
[21]	30–100	1024 bits	PSNR	Normalized (NC) and Cross (CC) Correlations	10	10 images in grayscale with 8 bit/pixel in depth	Cropping	Gaussian, Salt and pepper
[22]	10–100	16,384 bits	PSNR	NC	100	8 images in grayscale with 8 bit/pixel in depth	Rotation, Resizing, Cropping	Gaussian, Salt and pepper
[24]	10–100	16384 bits	-	2D Correlation Coefficient	10	1 image in grayscale with 8 bit/pixel in depth	Rotation, Scaling	Gaussian
[25]	75–100	1024 bits	PSNR	NC	-	2 images in grayscale with 8 bit/pixel in depth	Cropping	Gaussian, Salt and pepper, Speckle
[26]	70–100	1024 bits	PSNR	NC	100	4 images in grayscale with 8 bit/pixel in depth	Rotation, Cropping	Gaussian, Salt and pepper, Speckle
Proposed Method	20–100	32 bits	VIF	BCR	100	1000 images in color with 24 bit/pixel in depth	Rotation, Resizing, Cropping, Affine transformation, Translation, Shearing, Aspect ratio changes	Gaussian, Salt and pepper, Speckle

6. Conclusions

In this paper, we propose an improved robust watermarking algorithm in DFT transform via spread spectrum DS-CDMA, optimizing the key operation parameters, particularly the amounts of bands and coefficients of frequency as well as the watermark strength factor using the PSO optimization algorithm. This research reveals several findings related to the use of the PSO algorithm to improve the performance of an invisible watermarking scheme. One of these is related to the design of fitness function of PSO. In this way, we show that instead of continuing the mainstream of the state-of-the-art in the use of the metric PSNR in the fitness function of the PSO algorithm, we can employ another visual quality metric such as VIF, which reflects perceptual distortions more precisely than the PSNR, and can help to obtain better performance results in terms of imperceptibility. Another finding is related to the kind and number of attacks considered in the fitness function. Analyzing a priori the attacks and the tolerance against which the conventional invisible watermarking has weaknesses, the design of the fitness function can focus only on improving the robustness against these attacks, assuming that against other the watermarking will keep the robustness. Another finding is the focus of the state-of-the-art to increase the watermark payload neglecting the robustness against geometric distortions. Another critical finding is the few images considered in the testing performed by the current state-of-the-art, which may be a serious drawback to implement the watermarking algorithm in large-scale image datasets. In this way, a massive testing in terms of imperceptibility and robustness considering large image datasets should be compulsory, as in the case of our proposal that considers a dataset of 1000 color images with 24 bit/pixel resolution. Finally, in invisible watermarking, payload, imperceptibility, and robustness are not the only constraints to deal with but security is important too. To solve security issues in conventional DFT-based watermarking, the PSO algorithm has a fundamental role, finding the unique secret key to

each image in a given dataset, moreover it has benefits in terms of imperceptibility and robustness. As a future work, we will try improving the payload of our proposal, keeping the imperceptibility and robustness obtained hitherto.

Author Contributions: Conceptualization, M.C.-H. and A.C.-H.; Funding acquisition, F.J.G.-U.; Methodology, M.C.-H., A.C.-H. and F.J.G.-U.; Software, M.C.-H. and A.C.-H.; Supervision, M.C.-H.; Validation, M.C.-H.; Writing—original draft, M.C.-H.; Writing—review and editing, A.C.-H. and F.J.G.-U. All authors have read and agreed to the published version of the manuscript.

Funding: This research was funded by Consejo Nacional de Ciencia y Tecnología de México (CONACYT) grant number 161591, Instituto Politécnico Nacional (IPN) grant number SIP20210582 And The APC was funded by PAPIIT IT-101119 project research from DGAPA in the Universidad Nacional Autónoma de México (UNAM).

Institutional Review Board Statement: Not applicable.

Informed Consent Statement: Not applicable.

Data Availability Statement: No new data were created or analyzed in this study. Data sharing is not applicable to this article.

Acknowledgments: Authors would like to thank the Instituto Politécnico Nacional (IPN), the Tecnológico de Monterrey (ITESM), the PAPIIT IT-101119 project research from DGAPA in the Universidad Nacional Autónoma de México (UNAM), as well as the Consejo Nacional de Ciencia y Tecnología de México (CONACYT) by the support provided during the realization of this research.

Conflicts of Interest: The authors declare no conflict of interest.

References

1. Cox, I.J.; Miller, M.L.; Bloom, J.A.; Fridrich, J.; Kalker, T. *Digital Watermarking and Steganography*, 2nd ed.; Morgan Kaufmann Publisher: San Francisco, CA, USA, 2008.
2. Barni, M.; Bartolini, F. *Watermarking Systems Engineering: Enabling Digital Assets Security and Other Applications*; Marcel Dekker: New York, NY, USA, 2004.
3. Jia, L.; Kumar, S. Robust Digital Watermarking Techniques for protecting copyright Applied to Digital Data: A Survey. *Turk. J. Comp. Math. Educ.* **2021**, *12*, 3819–3825.
4. Tao, H.; Chongmin, L.; Mohamad Zain, J.; Abdalla, N. Robust Image Watermarking Theories and Techniques: A Review. *J. Appl. Res. Technol.* **2014**, *12*, 122–138. [[CrossRef](#)]
5. Kennedy, J.; Eberhart, R. Particle swarm optimization. In Proceedings of the ICNN'95—International Conference on Neural Networks, Perth, WA, Australia, 27 November 1995; IEEE: Piscataway, NJ, USA, 1995; Volume 4, pp. 1942–1948.
6. Cedillo-Hernandez, M.; Cedillo-Hernandez, A.; Garcia-Ugalde, F.; Nakano-Miyatake, M.; Perez-Meana, H. Digital color images ownership authentication via efficient and robust watermarking in a hybrid domain. *Radioengineering* **2017**, *26*, 536–551. [[CrossRef](#)]
7. Dubendorf, V.A. *Wireless Data Technologies*; John Wiley & Sons, Ltd.: Hoboken, NJ, USA, 2003.
8. Solachidis, V.; Pitas, I. Circularly symmetric watermark embedding in 2-D DFT domain. *IEEE Trans. Image Process.* **2001**, *10*, 1741–1753. [[CrossRef](#)]
9. Hernandez, M.C.; Miyatake, M.N.; Meana, H.M.P. Analysis of a DFT-based watermarking algorithm. In Proceedings of the 2nd International Conference on Electrical and Electronics Engineering, Mexico City, Mexico, 9 September 2005; IEEE: Piscataway, NJ, USA, 2005; pp. 44–47.
10. Cedillo-Hernández, M.; García-Ugalde, F.; Nakano-Miyatake, M.; Pérez-Meana, H.M. Robust hybrid color image watermarking method based on DFT domain and 2D histogram modification. *Signal Image Video Process.* **2014**, *8*, 49–63. [[CrossRef](#)]
11. Cedillo-Hernández, M.; García-Ugalde, F.; Nakano-Miyatake, M.; Pérez-Meana, H.M. Robust watermarking method in DFT domain for effective management of medical imaging. *Signal Image Video Process.* **2014**, *9*, 1163–1178. [[CrossRef](#)]
12. Sun, X.C.; Lu, Z.M.; Wang, Z.; Liu, Y.L. A geometrically robust multi-bit video watermarking algorithm based on 2-D DFT. *Multimed. Tools Appl.* **2021**, *80*, 13491–13511. [[CrossRef](#)]
13. Ying, Q.; Lin, J.; Qian, Z.; Xu, H.; Zhang, X. Robust digital watermarking for color images in combined DFT and DT-CWT domains. *Math. Biosci. Eng.* **2019**, *16*, 4788–4801. [[CrossRef](#)] [[PubMed](#)]
14. Wang, X.Y.; Hou, L.M.; Wu, J. A feature-based robust digital image watermarking against geometric attacks. *Image Vision Comput.* **2008**, *26*, 980–989. [[CrossRef](#)]
15. Nuñez-Ramirez, D.; Cedillo-Hernandez, M.; Nakano-Miyatake, M.; Perez-Meana, H. Efficient Management of Ultrasound Images using Digital Watermarking. *IEEE Lat. Am. Trans.* **2020**, *18*, 1398–1406. [[CrossRef](#)]
16. Cedillo-Hernandez, M.; Garcia-Ugalde, F.; Nakano-Miyatake, M.; Perez-Meana, H. Robust Object-Based Watermarking Using SURF Feature Matching and DFT Domain. *Radioengineering* **2013**, *22*, 1057–1071.

17. Jung, Y.J.; Kang, H.K.; Ro, Y.M. Novel watermark embedding technique based on human visual system. In Proceedings of the Security and Watermarking of Multimedia Contents III: Proceedings of Spie, San Jose, CA, USA, 22–25 January 2001; Volume 4314, pp. 475–482.
18. Zhang, L.; Wei, D. Robust and reliable image copyright protection scheme using down sampling and block transform in integer wavelet domain. *Digit. Signal Process.* **2020**, *106*, 102805. [[CrossRef](#)]
19. Kang, X.; Chen, Y.; Zhao, F.; Lin, G. Multi-dimensional particle swarm optimization for robust blind image watermarking using intertwining logistic map and hybrid domain. *Soft Comput.* **2020**, *24*, 10561–10584. [[CrossRef](#)]
20. Hsu, L.Y.; Hu, H.T. Blind watermarking for color images using EMMQ based on QDFT. *Expert Syst. Appl.* **2020**, *149*, 1–16. [[CrossRef](#)]
21. Ahmadi, S.B.B.; Zhang, G.; Wei, S.; Boukela, L. An intelligent and blind image watermarking scheme based on hybrid SVD transforms using human visual system characteristics. *Visual Comput.* **2021**, *37*, 385–409.
22. Zhang, L.; Wei, D. Dual DCT-DWT-SVD digital watermarking algorithm based on particle swarm optimization. *Multimed. Tools Appl.* **2019**, *78*, 28003–28023. [[CrossRef](#)]
23. Riadi, S.; Triono, S.; Syahril, S.; Nofriansyah, D. A Novel Security based Image Watermarking using NBP-IWT-DCT-NSVD-GA-PSO Algorithm. *Int. J. Eng. Adv. Technol.* **2019**, *9*, 1600–1609.
24. Thakkar, F.N.; Srivastava, V.K. Performance comparison of recent optimization algorithm Jaya with particle swarm optimization for digital image watermarking in complex wavelet domain. *Multidimens. Syst. Signal Process.* **2019**, *30*, 1769–1791. [[CrossRef](#)]
25. Zhou, N.R.; Luo, A.W.; Zou, W.P. Secure and robust watermark scheme based on multiple transforms and particle swarm optimization algorithm. *Multimed. Tools Appl.* **2019**, *78*, 2507–2523. [[CrossRef](#)]
26. Takore, T.T.; Kumar, P.R.; Devi, G.L. A New Robust and Imperceptible Image Watermarking Scheme Based on Hybrid Transform and PSO. *Int. J. Intell. Syst. Appl.* **2018**, *11*, 50–63. [[CrossRef](#)]
27. Zheng, Z.; Saxena, N.; Mishra, K.; Sangaiah, A.K. Guided dynamic particle swarm optimization for optimizing digital image watermarking in industry applications. *Future Gener. Comput. Syst.* **2018**, *88*, 92–106. [[CrossRef](#)]
28. Shih, F.Y.; Zhong, X.; Chang, I.C.; Satoh, S. An adjustable-purpose image watermarking technique by particle swarm optimization. *Multimed. Tools Appl.* **2018**, *77*, 1623–1642. [[CrossRef](#)]
29. Sheikh, H.R.; Bovik, A.C. Image information and visual quality. *IEEE Trans. Image Process.* **2006**, *15*, 430–444. [[CrossRef](#)]
30. Lin, T.Y.; Maire, M.; Belongie, S.; Hays, J.; Perona, P.; Ramanan, D.; Dollár, P.; Zitnick, C.L. Microsoft COCO: Common objects in context. In *Proceedings of the European Conference on Computer Vision*; Springer International Publishing: Cham, Switzerland, 2014; pp. 740–755.
31. Chareyron, G.; Da Rugna, J.; Tremeau, A. Chapter 3: Color in Image Watermarking. In *Advanced Techniques in Multimedia Watermarking: Image, Video and Audio Applications*; Information Science Reference: Hershey, PA, USA, 2010; pp. 36–56.
32. Trémeau, A.; Tominaga, S.; Plataniotis, K.N. Color in Image and Video Processing: Most Recent Trends and Future Research Directions. *EURASIP J. Image Video Process.* **2008**, *3*, 1–26. [[CrossRef](#)]
33. Tang, C.W.; Hang, H.M. A feature-based robust digital image watermarking scheme. *IEEE Trans. Signal Process.* **2003**, *51*, 950–959. [[CrossRef](#)]
34. Cayre, F.; Fontaine, C.; Furon, T. Watermarking security: Theory and practice. *IEEE Trans. Signal Process.* **2005**, *53*, 3976–3987. [[CrossRef](#)]